

**Lunar domes near Lansberg D: Morphometry and mode of formation.** M. Wirths<sup>1</sup> and R. Lena<sup>2</sup> - Geologic Lunar Research (GLR) Group. <sup>1</sup>km 67 Camino Observatorio, Baja California, Mexico; [mwirths@starband.net](mailto:mwirths@starband.net); <sup>2</sup> Via Cartesio 144, sc. D, 00137 Rome, Italy; [r.lena@sanita.it](mailto:r.lena@sanita.it)

**Introduction:** In this contribution we provide an analysis of three domes located near Lansberg D. The first dome, termed Lansberg 1 (La1), is located at 29.79° W and 3.54° S and has an elongated base area of 20 x 16 km<sup>2</sup> (cf. Fig. 1).

The second examined dome, termed Lansberg 2 (La2), is located to the south of La1 at 30.23° W and 4.02° S and has an elongated base area of 25 x 19 km<sup>2</sup>. It is clearly apparent in Fig. 1 that both domes are characterised by several straight rilles traversing their surfaces and by small non-volcanic hills. Another dome, which we termed Lansberg 3 (La3), is located at 30.09° W and 4.49° S, and has an elongated base area of 19 x 15 km<sup>2</sup>. These flat domes are clearly detectable in the WAC imagery (Fig. 1c).

It is unlikely that they are kipukas as no spectral contrast is apparent between them and the surrounding surface. Similar to previously examined lunar domes of presumably intrusive origin [1-2], three domes near Lansberg D are of strongly elongated shape and La1

and La2 display straight rilles traversing their surfaces, which are likely of tensional origin, due to a possible intrusive origin [1-2].

**Morphometric properties:** Based on the telescopic CCD image, which was acquired under oblique solar illumination, we determined DEMs of the examined domes by applying the combined photoclinometry and shape from shading method described in [3], (Figs. 2 and 3). The heights and flank slopes of the domes were extracted from the DEMs. We also have determined surface elevations by GLD100 dataset [4], which are in good agreement with our image-based photoclinometry and shape from shading analysis (Fig. 3).

The heights of La1-La3 correspond to 120 m, 80 m and 120 m, respectively, resulting in average flank slopes of 0.68°, 0.40° and 0.77°.

The domes volumes were estimated by assuming a parabolic dome shape, resulting in edifice volumes of about 19 km<sup>3</sup>, 17 km<sup>3</sup> and 15 km<sup>3</sup>, respectively.

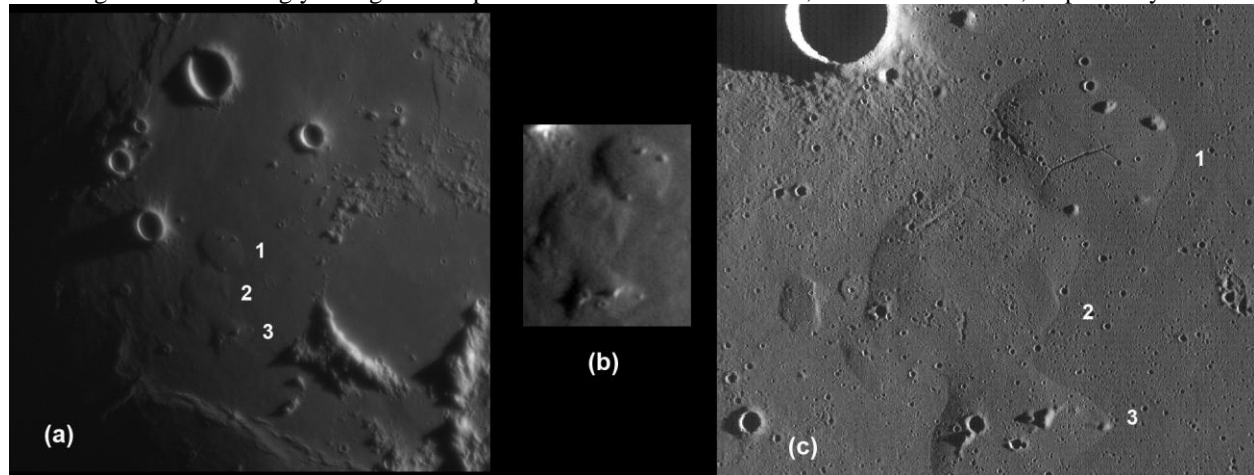


**Fig. 1.** (a) Telescopic CCD image acquired on January 22, 2013 01:49 UT with a 400 mm aperture Starmaster driven Dobsonian (Wirths); (b) Rectified view of the telescopic CCD image; (c) Crop of the LRO WAC imagery M116507209ME.

**Laccolith modelling:** Both domes show the characteristic non-circularity of the outlines of the candidate intrusive domes [1-2]. If we assume that the linear rilles on the surfaces of La1 and La2 are the result of tensional stress, the curvature radii of the dome surfaces inferred from our 3D analysis yield thicknesses of the uppermost mare basalt layer of at least 0.15 and 1.1 km, respectively, assuming a typical value of the critical stress of basalt of 13 MPa [5]. The laccolith model in [6] applied according to the numerical scheme suggested in [1] yields intrusion depths of 1.0 km and 2.5

km and maximum magma pressures in the laccolith of 7.9 MPa and 20 MPa, respectively.

The inferred intrusion depth and magma pressure of La3 amounts to 0.79 km and 6.1 MPa, while the thicknesses of the uppermost mare basalt layer corresponds to 0.12 km.

The intrusion depth and magma pressure obtained for La1 are lower than values inferred for other putative intrusive domes of class In1 introduced in [1-2]. According to the laccolith model, these lower values are mainly a result of the smaller size of La1.

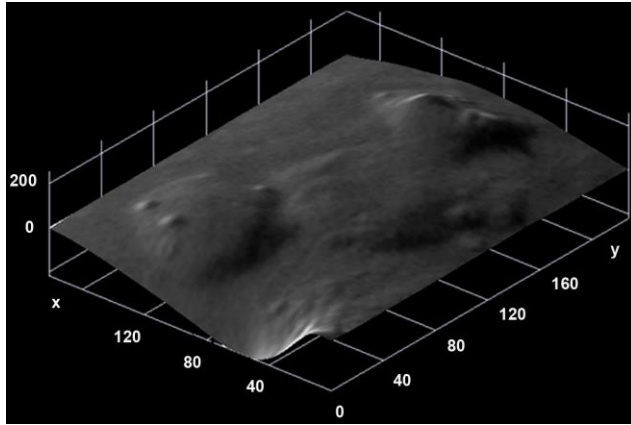


**Fig. 2:** 3D reconstruction obtained from the DEM, with the original CCD telescopic image superimposed on the elevation model. The region is seen from northwestern direction. The vertical axis is 10 times exaggerated.

**Conclusion:** The three low and large examined lunar domes are interpreted as being formed by magmatic intrusion. Regarding the morphometric properties and modelling results, La2 and La3 are typical representative of class In1 and In2, respectively.

The steeper dome La3 indicates that laccolith formation proceeded until the stage characterized by flexure of the overburden, while La2 and La1 are characterized by rilles likely due to tensional stresses, consistent with laccolith formation. Hence the magma accumulating beneath the surface produced not only an upbowing of the surface rock layers but also failures in the rock strata (fracturing).

The intrusion depth and magma pressure inferred for La1 is lower limit of the range of previously modelled values of class In1 domes [2] by factors of about 2–3.

**References:** [1] Wöhler & Lena (2009) *Icarus* 204, 381-398; [2] Lena et al. (2013) *Lunar Domes: Properties and Formation Processes*. Springer Praxis Books; [3] Wöhler et al. (2006) *Icarus* 183, 237-264; [4] Scholten et al. (2012) *J. Geophys. Res.* 117 (E00H17), doi:10.1029/2011JE003926; [5] Pollard and Fletcher (2005), *Fundamentals of Structural Geology*, Cambridge University Press; [6] Kerr and Pollard (1998), *J. Struct. Geol.* 20 (12).

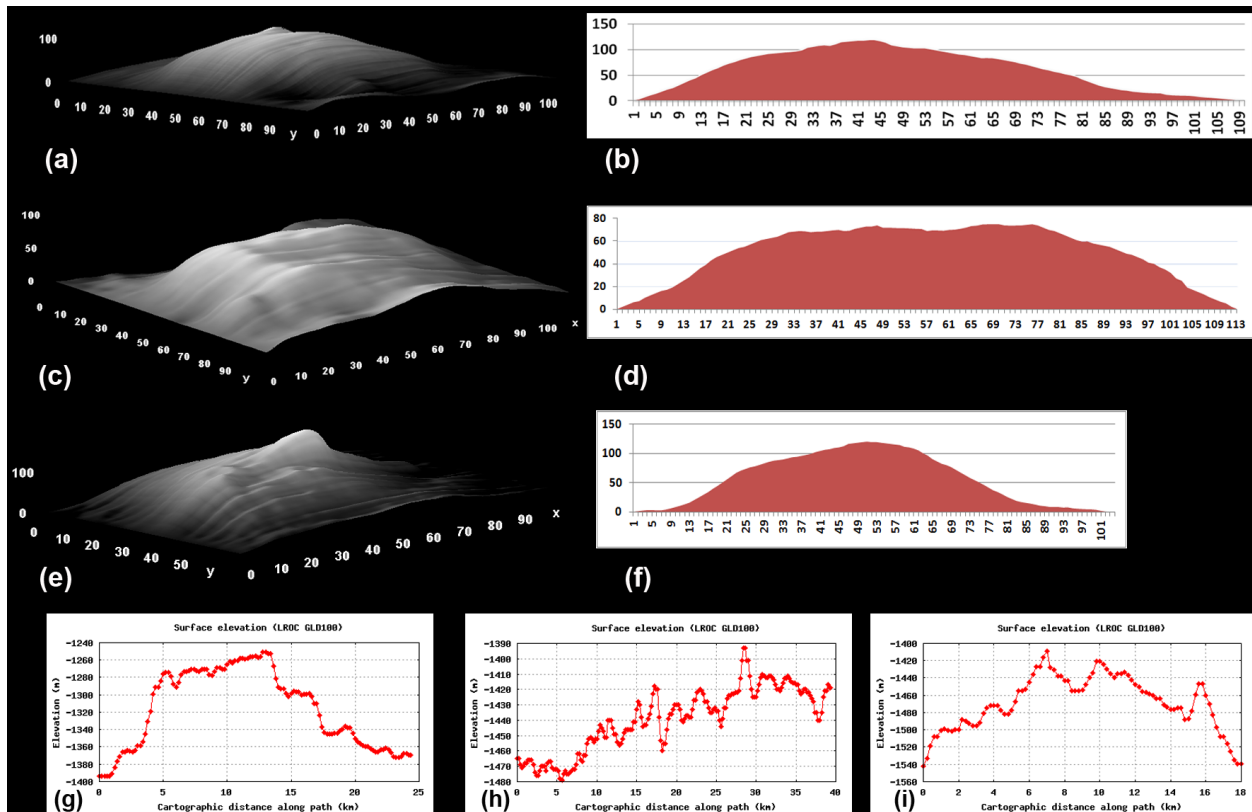


**Fig. 3.** 3D reconstruction and cross-sectional profile in east-west direction derived for (a-b) La1 dome, (c-d) La2 and (e-f) La3. The vertical axis is 10 times exaggerated. (g-i) Cross-sectional profile in east-west direction based on GLD100 dataset for the three examined domes La1-La3, respectively.